Available online at www.sciencedirect.com
ScienceDirect
Polymer 48 (2007) 5653–5661
polymer
www.elsevier.com/locate/polymer

Control of electrospun mat width through the use of parallel auxiliary electrodes

Yiquan Wu [a,b], Lisa A. Carnell [a,b,c], Robert L. Clark [a,b,*]

[a] Center for Biologically Inspired Materials and Material Systems, Duke University, Durham, NC 27708, USA
[b] Mechanical Engineering and Materials Science, Pratt School of Engineering, Duke University, Durham, NC 27708, USA
[c] NASA Langley Research Center, Hampton, VA 23681, USA

Received 17 May 2007; received in revised form 5 July 2007; accepted 6 July 2007
Available online 18 July 2007

Abstract

Electrospinning offers a versatile way to produce one-dimensional micrometer or nanometer materials; however, electrospun fibers are typically collected in a random orientation limiting their applications. In the present study, we have expanded upon a technique used to align fibers for control of the fiber distribution during the spinning process through the use of auxiliary counter electrodes. The electrostatic force imposed by the auxiliary electrodes provides a converged electric field, which affords control over the distribution of the fibers on the rotating collector surface. Experimental results demonstrate that the width of electrospun mats can be decreased dramatically when parallel auxiliary electrodes are employed at the collector. There was no apparent difference in the average diameters of the electrospun fibers as a result of the additional auxiliary electrodes, but the fiber distribution density in terms of mat width was greatly improved. Thus, the use of auxiliary counter electrodes at the rotating collectors provides a viable method of converging and controlling the deposition of electrospun fibers.

Keywords: Electrospinning; Aligned fiber; Poly(ε-caprolactone)

1. Introduction

Recently, electrospinning has attracted significant attention as a manufacturing process for producing one-dimensional materials with diameters ranging from the micrometer to nanometer scales [1–3]. The technique provides a promising and straightforward way to fabricate infinite and continuous fibers applied as nanostructured and biomedical materials [4–6]. A wide range of materials such as biological polymers, engineered polymers, ceramics and composites has been successfully electrospun into one-dimensional materials having many different microstructures [7–9]. Applications of electrospun materials in nanotechnology include tissue scaffolds, fibers for drug delivery, composite reinforcement, chemical sensing, enzyme immobilization, membrane-based filtration, protective clothing, catalysis, solar cells, electronic devices and others [10–15].

Electrospinning involves the application of electrostatic force instead of mechanical force to atomize liquid solution into charged aerosol jets [16]. In a typical electrospinning process, firstly a precursor solution is held at the tip of the nozzle in the form of a droplet by its surface tension, and then a charge is induced on the surface of the droplet when a high voltage is applied to the metallic nozzle. Finally, with an increase of the electric field above a critical voltage for which the electrohydrodynamic force within the charged droplet is larger than its surface tension, the droplet is distorted and a jet will erupt from the apex of a conical meniscus, commonly known as the Taylor-cone [17]. The charged jets move toward the sample collector while most of the solvents evaporate, resulting in solid fiber materials. Although, the jets in a Taylor-cone mode are stable near the tip of the nozzle, the electrospun fibers experience a fluid instability stage that leads

* Corresponding author. Mechanical Engineering and Materials Science, Pratt School of Engineering, Duke University, Durham, NC 27708, USA. Tel.: +1 919 660 5435; fax: +1 919 660 5409.
E-mail address: rclark@duke.edu (R.L. Clark).

0032-3861/$ - see front matter © 2007 Elsevier Ltd. All rights reserved.
doi:10.1016/j.polymer.2007.07.023

to solidification of the jet and thinning of fibers while the jets approach the collector [18]. It is due to this fluid instability that the electrospun fibers are often collected as randomly oriented structures in the form of non-woven mats lacking structural orientation.

However, significant interest exists in obtaining the aligned electrospun fibers to fabricate devices with unique electrical, optical and mechanical properties for some applications such as blood vessels, microelectronics, and photonics, which often require well-aligned and highly ordered architectures [19–21]. Moreover, aligned electrospun fibers have a variety of potential applications in other fields, including reinforced composite materials, electrochemical sensors and bioengineering [22–24]. The challenges of generating aligned electrospun fibers have been met with some successes by using an electrostatic field and a rotating mechanical drum [25–26]. The electrospun fibers can be aligned when a drum rotating or a wheel-like bobbin is used as the collector [27–28]. There have been several reported successes of aligning fibers through the use of patterned collectors arranged in a particular angle with a certain gap, because the electrospun fibers can be aligned across the patterned electrodes [29–30]. Aligned fibers have also be obtained through the simultaneous application of a rotating drum and counter electrode at the collector [31], and by employing an electrostatic lens to stabilize and focus the charged jets to generate oriented fibers [32].

In this paper, we report a modified electrospinning process that can be used to control the width of aligned fiber mats by converging the charged jets with the help of auxiliary electrodes. It is similar to the setup described in the work by Carnell et al. [31] where a conventional rotating collector is employed with the addition of an auxiliary electrode positioned directly behind the collector to direct the fiber orientation; however, we have added two additional auxiliary electrodes to assist in converging the electric field to control the width of the final mat generated.

2. Experimental

Fig. 1 illustrates a schematic setup used for generating aligned electrospun fibers with controlled mat width. As influenced by the auxiliary electrostatic field, the electrospun fibers were focused between the gaps of the two electrostatic field electrodes to form parallel fibers, which were collected conveniently onto the rotating collector. The counter electrode opposite to the spinning nozzle is designed to stretch the charged electrospun fibers by forming a strong electrostatic field between the nozzle and collector. All the electrodes are in the same plane as the top surface of the drum.

A biodegradable polymer solution of 8 w/v% was prepared by dissolving poly(ε-caprolactone) (Aldrich) in a solvent mixture composed of dichloromethane and methanol (Aldrich) in a ratio of 7:3 by volume. The solution was mixed thoroughly using a magnetic stirring bar. The polymer solution was loaded in a 10-ml plastic syringe (BD company) equipped with a stainless steel nozzle (McMaster), and was continuously forced through the nozzle using a syringe pump (Cole–Parmer) at a constant rate of 2.5 ml/h. The nozzle was connected to a high-voltage power supply (Acopian) that is capable of generating voltages up to 30 kV. The three auxiliary electrodes were also connected to different power supply (Gamma High Voltage Research Inc) to generate a converged electrostatic field. The collector rotated at a speed of 1000 rpm and was located 15 cm away from the nozzle. The surface velocity of drum was analyzed in a range of 0.5–4.0 m/s to determine an appropriate take-up velocity. Fig. 2 shows a schematic diagram to illustrate the designations of the processing parameters in the experiment. The key processing parameters are shown in Table 1. After electrospinning for 30 min, a fibrous mat collected perpendicular to the collector axis was observable. The electrospun mats prepared with different conditions were imaged using a digital camera (Canon Inc). The microstructures and morphologies of electrospun fibers were characterized using a field-emission scanning electron microscope (FE-SEM, Philips XL 30 SEM, Netherlands) operated at an accelerating voltage of 5 kV. The samples were coated with gold before SEM imaging. The fiber diameters and the angular distribution of the aligned fibers were quantitatively measured and analyzed from high-magnification SEM micrographs (FEI XL 30 SEM-FEG).

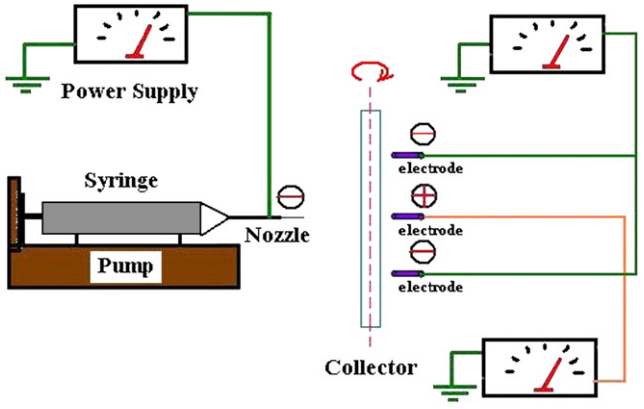

Fig. 1. Schematic illustration setup of the focused electrospinning with three auxiliary electrodes.

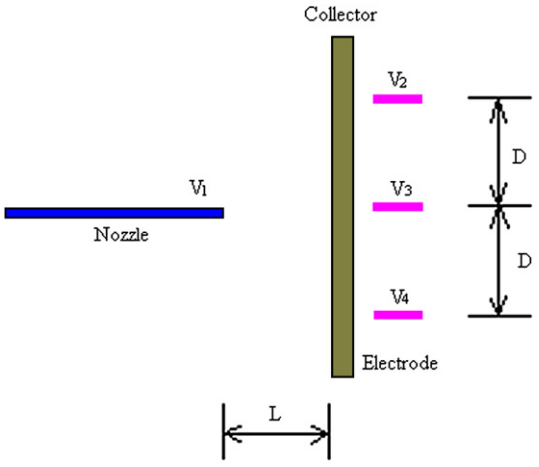

Fig. 2. Schematic diagrams to illustrate the designations of processing parameters.

Table 1
Processing parameters of focused electrospinning

	V_1 (kV)	V_2 (kV)	V_3 (kV)	V_4 (kV)	D (cm)	L (cm)	F (ml/h)	C (w/v)	S (rpm)
(a)	−15	0	0	0	0	15	2.5	8	1000
(b)	−15	0	+8	0	0	15	2.5	8	1000
(c)	−15	−10	+8	−10	5.0	15	2.5	8	1000
(d)	−15	−10	+8	−10	2.5	15	2.5	8	1000

V: Voltage; D: electrode distance; L: spinning distance; F: flow rate of solution; C: concentration; S: speed of rotating collector.

3. Results and discussion

Five different surface velocities of the drum between 0.5 m/s and 4 m/s were tested for optimizing the surface velocity of the collector to match the velocity of the jet by applying a counter auxiliary electrode behind the drum. Fig. 3(a)–(d) show SEM micrographs of the electrospun fibers prepared using different drum surface velocity. When the surface velocity was 0.5 m/s, the electrospun fibers were almost randomly distributed in the mat, as shown in Fig. 3(a). It is believed that the velocity of the electrospun jet was higher than surface velocity of drum. Fig. 3(b) shows that as the surface velocity of drum was increased to 1.0 m/s, the alignment of the electrospun fibers was enhanced but still had some electrospun fibers distributed randomly. This is because when the velocity of the jet was higher than the surface velocity of drum, the electrospun fibers could not be taken-up at a matching velocity by the drum due to the higher jet velocity. When the surface velocity of drum was 2.0 m/s, most of the electrospun fibers were aligned along one direction without being stretched, as shown in Fig. 3(c). This is attributed to the fact that the velocity of the electrospun jet was close to the surface velocity of the drum. As the surface velocity of the drum was increased to 3.0 m/s and 4.0 m/s, the electrospun fibers were collected onto the drum in an aligned state but were thinned (Fig. 3(d)) and stretched to break (Fig. 3(e)). This is because the surface velocity of drum was higher than the velocity of the electrospun jet. Therefore, the electrospun fibers were collected and stretched by the drum with a high surface velocity and were broken at a higher surface velocity. It was concluded from the experiment that the surface velocity of drum at 2.0 m/s was an appropriate take-up velocity for the electrospun PCL jets in the experiment.

Fig. 4(a)–(d) shows digital images of electrospun mats using different parameters listed in Table 1. The image in Fig. 4(a) reveals that the electrospun fibers are not aligned well by only rotating the collector. Although, the rotation can assist the alignment of the electrospun fibers, it is still not easy to achieve a well-aligned assembly of the fibers. As detailed by Carnell et al. [31], when an auxiliary counter electrode is used to assist the orientation of fibers, the extent of alignment of electrospun fibers can be increased, as shown in Fig. 4(b). When incorporating multiple electrodes, as was the case for the results shown in Fig. 4(c) and (d), the electrospun fibers on the mats exhibit both alignment and controlled width. This was attributed to the electric force that focused and aligned the electrospun jets when they were on the passage to the collector under an electrostatic field. When only one auxiliary counter electrode was used behind the collector to assist the alignment of the fibers, an aligned mat with a width of 6.0 cm could be produced. However, when two additional auxiliary counter electrodes were used with the counter electrode simultaneously, the assembly of the

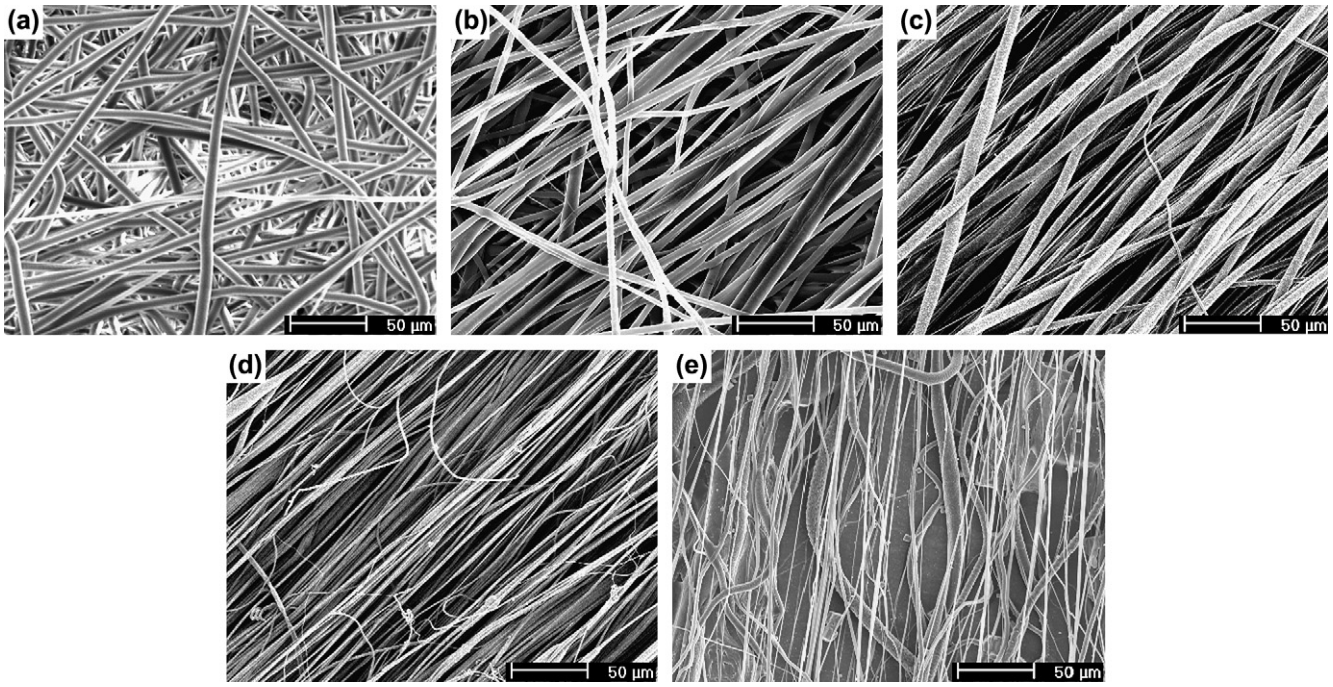

Fig. 3. SEM micrographs of PCL mats prepared using a counter auxiliary electrode at different surface velocity: (a) 0.5 m/s; (b) 1.0 m/s; (c) 2.0 m/s; (d) 3.0 m/s and (e) 4.0 m/s.

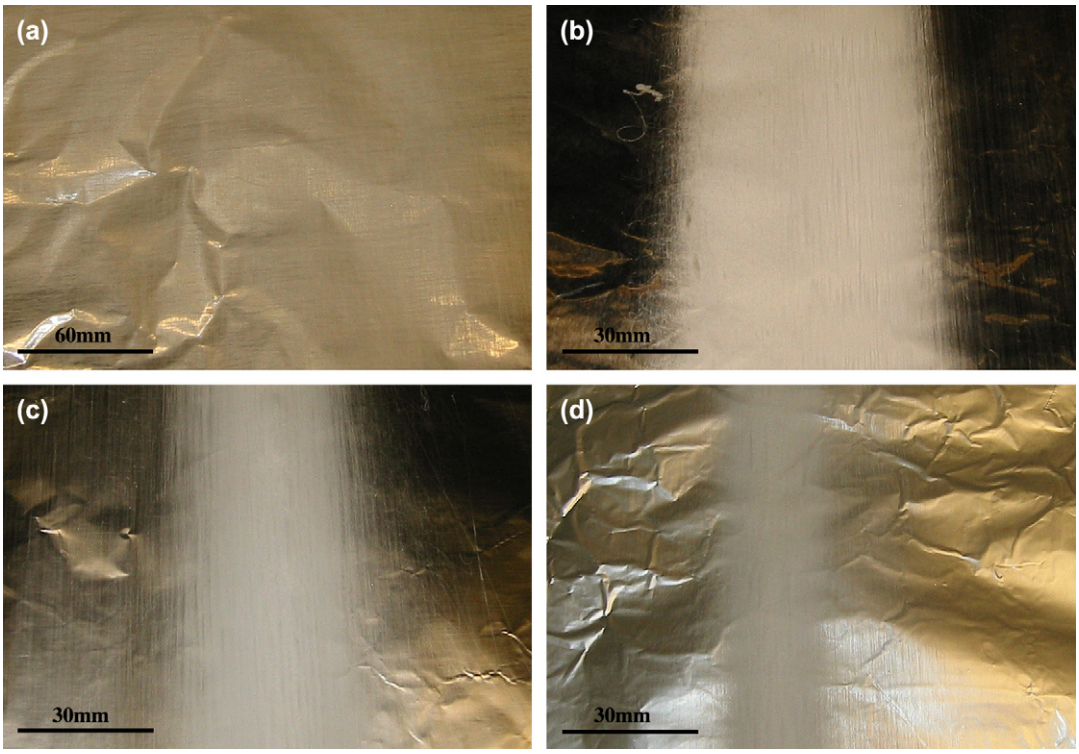

Fig. 4. Digital images of electrospun mats prepared with differently designed electrodes: (a) no auxiliary electrodes; (b) one counter auxiliary electrode; (c) and (d) three auxiliary electrodes with different separation distances.

electrospun fibers was aligned and focused, as shown in Fig. 4(c) and (d). The width of the electrospun mats was narrowed from 4.6 cm to 2.2 cm as the distance, D, between the electrodes was decreased from 5.0 cm to 2.5 cm, as shown in Fig. 4(c) and (d). As the distance is decreased, the auxiliary electrodes serve to further focus the electrostatic field and constrain the deposition of the electrospun fibers.

Table 2 lists the densities of electrospun fibers of the mats prepared using the conditions (a)–(d). Density, expressed in unit of N/cm (number of fibers per centimeter), increased from 2.0 N/cm to 4.2 N/cm as the width of electrospun mats decreased from 2.4 cm to 2.2 cm. The density increase was not inversely proportional to the decrease of mat width, because the electrospun fibers were assembled in different layers. The experiment showed that the voids within the electrospun mats were formed through the overlaying of fibers during electrospinning. By converging the electric field through the use of multiple electrodes, the aligned, electrospun fibers and resulting mats exhibited a denser microstructure and lower porosity when compared to non-woven mats. This was due to the electrostatic force that resulted from the auxiliary electrodes that converged and assembled the fibers in a focused mode. The rotating collector only resulted in a density of 2.0 N/cm. When a counter electrode was employed, the density was increased to 2.5 N/cm. However, when three auxiliary electrodes were applied simultaneously, the densities were increased from 2.5 N/cm to 3.8 N/cm and 4.2 N/cm for the electrode distances of 5.0 cm and 2.5 cm, respectively. The results demonstrated that the alignment and density of the electrospun fiber could be improved with the help of a converged electric field by using auxiliary electrodes.

Fig. 5 shows SEM micrographs of the electrospun mats prepared in the conditions (a)–(d). The electrospun fibers prepared in condition (a) do not reveal good aligned structure when compared to the fibers obtained in conditions (b)–(d), in which most of the fibers are aligned and oriented perpendicular to the axis of the rotating collector. The diameters of fibers in the mat prepared in condition (a) range from 5.0 μm to 8.0 μm, with an average diameter of 6.7 ± 0.4 μm (see Fig. 5(a)) while the fiber diameters of the mats prepared in condition (b) vary from 1.1 μm to 9.8 μm, with an average diameter of 7.1 ± 0.2 μm, when a counter electrode was used (see Fig. 5(b)). The SEM image of electrospun fibers achieved in condition (d) shows better orientation and alignment than that achieved in condition (c). The diameters of fibers in the electrospun mat produced in condition (c) are in a range of 0.83–11.7 μm, having an average diameter approximately of 7.0 ± 0.2 μm (see Fig. 5(c)). When the separation distance between electrodes, D, was reduced to 2.5 cm, the diameters

Table 2
Analysis of electrospun fibers in mats prepared in different conditions

	(a)	(b)	(c)	(d)
D (cm)	0	0	5.0	2.5
W (cm)	24	6.0	4.6	2.2
d (N/cm)	2.0	2.5	3.8	4.2
$P_{\theta(80°-90°)}$	19.6	55.8	59.5	72.5

W: Width of the electrospun mats; d: density of fibers; $P_{\theta(80°-90°)}$: percentage of fiber with a aligned angle in 80°–90°.

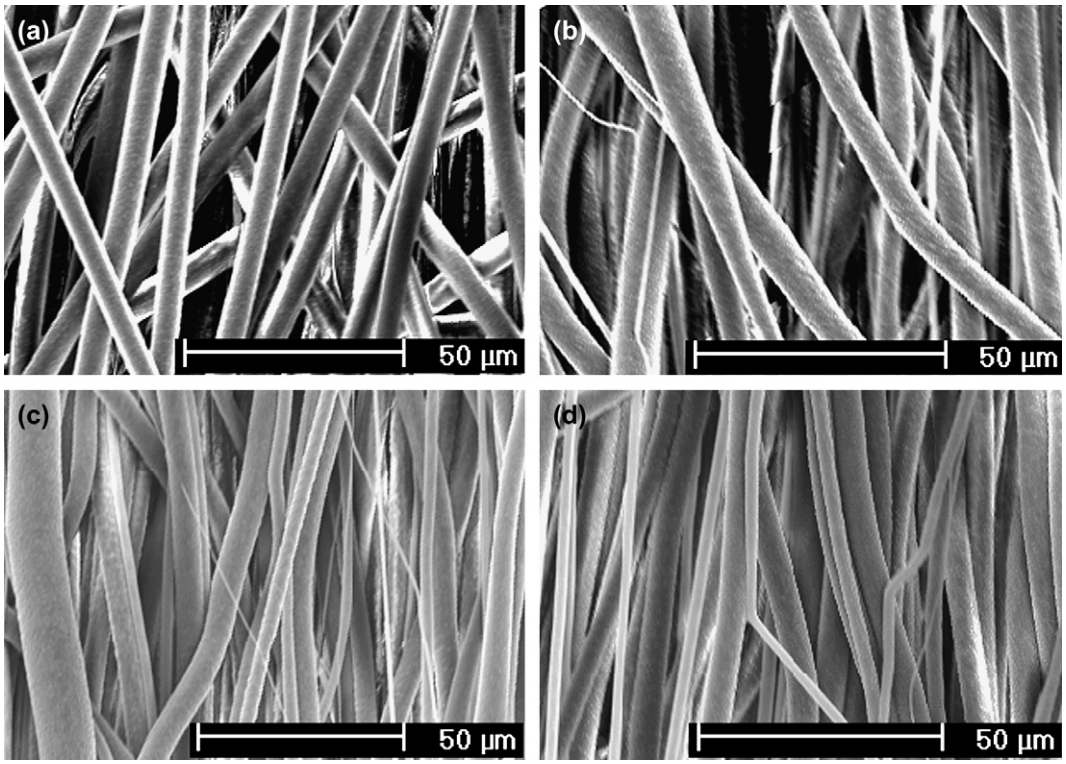

Fig. 5. SEM images of electrospun mats prepared with differently designed electrodes: (a) no auxiliary electrodes; (b) one counter auxiliary electrode; (c) and (d) three auxiliary electrodes with different separation distances.

of electrospun fibers ranged from 1.0 μm to 11.1 μm, with an average diameter of 6.5 ± 0.3 μm (see Fig. 5(d)). These results demonstrate that the fiber alignment increased as the distance between the auxiliary electrodes decreased, but the diameters of fibers were not influenced distinctly by the auxiliary electrodes. The improvement of fiber distribution and alignment was attributed to the converged electric fields formed by using the three auxiliary electrodes.

Fig. 6 shows percentage of measured fiber diameters as prepared in conditions (a)–(d). The diameters of fibers in the mat prepared in condition (a) are analyzed and characterized in the range from 4.9 μm to 8.1 μm. Most of the fiber diameters are scattered in a narrow distribution between 5.7 μm and 8.1 μm. The distribution of fiber diameters between 6.5 μm and 7.3 μm has the highest percentage, 56.6% ± 0.5%, as shown in Fig. 6(a). Fig. 6(b) reveals that the greatest distribution of fiber diameters ranges from 4.2 μm to 8.4 μm when a single counter electrode was used, with the highest percentage (25.0% ± 0.5%) in the range of 5.6–7.0 μm. When three auxiliary electrodes were used simultaneously, most of the fiber diameters in the electrospun mats produced in condition (c) were distributed between 3.4 μm and 8.5 μm, having 36.2% ± 0.2% of the fibers between 5.1 μm and 6.5 μm, as shown in Fig. 6(c). When the distance between electrodes, D, was reduced to 2.5 cm, the diameter distribution of electrospun fibers slightly broadened to a small diameter range, varying from 1.4 μm to 7.0 μm, as shown in Fig. 6(d). Fiber diameters ranging from 5.6 μm to 7.0 μm resulted in the highest percentage, 27.7% ± 0.4%. The experiment also shows that the average diameters decreased from 7.0 ± 0.2 μm to 6.5 ± 0.3 μm with decreasing electrode separation distance. The slight reduction in the average fiber diameter was believed to result from the additional stretching of the electrospun fibers caused by the converged electrostatic force formed from the auxiliary electrodes. Table 3 shows the standard deviation of the diameter distribution fraction for the electrospun fibers prepared using the conditions (a)–(d).

To characterize the alignment of the electrospun fibers, a statistical analysis of the angles between the long axes of the fibers and the axes of rotating collector was determined from the SEM images. The distributions of angles are shown in Fig. 7. It can clearly be seen that the degree of alignment of the electrospun fibers was increased, with the help of the auxiliary electrodes to enhance the orientation of the fibers. Fig. 7(a) reveals that the aligned angle distributions are scattered in a range of 0°–90° for the electrospun mat prepared with condition (a). Good alignment could be achieved when a counter electrode was applied, having an aligned angle distribution in a range of 40°–90°, as shown in Fig. 7(b). Fig. 7(c) and (d) shows a modest improvement in electrospun fiber alignment when additional auxiliary electrodes were used to further converge the electric field. Primarily, one observes less scatter in angle distribution as additional electrode are added and the separation between electrodes is decreased. The majority of fibers prepared in condition (a) have an angle distribution in the range of 50°–90°, while the distribution shifts to the region of 80°–90° for mats prepared in condition (d), reaching a fraction of 72.5% ± 0.4%. This shift was

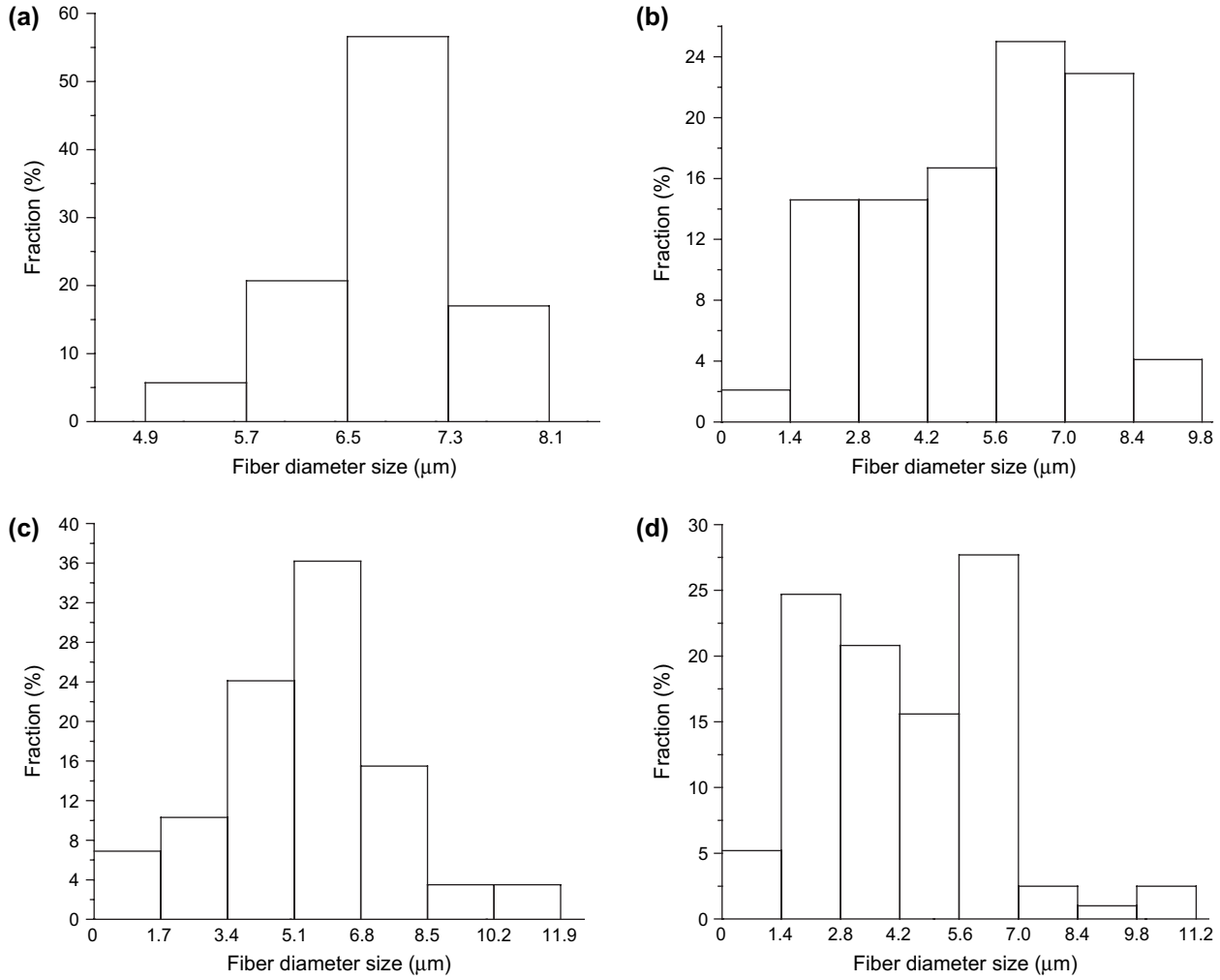

Fig. 6. Histogram of fiber diameter distribution of mats prepared with differently designed electrodes: (a) no auxiliary electrodes; (b) one counter auxiliary electrode; (c) and (d) three auxiliary electrodes with different separation distances.

attributed to the converged electric field to orient the fibers with the help of auxiliary electrodes in the electrospinning process. The percentages of fibers with an aligned angle in the range of 80°–90° for the mats prepared with different conditions are listed in Table 2. The standard deviations of the fraction for the aligned angle distribution are shown in Table 4.

When the diameter of the electrospun PCL fibers reduced to sub-micro regions, the alignment effects imposed by the auxiliary electric field formed the same distribution patterns as that in the electrospun mats having a micrometer fiber structure. The nanostructured PCL fibers were generated by using a diluted solution with a concentration of 3 w/v%. The nanostructured mats, consisting of PCL fibers having an average diameter of 570 ± 20 nm, could still be aligned and converged when three auxiliary electrodes were employed. SEM micrograph in Fig. 8(a) shows that the electrospun PCL fibers did not demonstrate a good aligned structure

Table 3
Standard deviation of the fraction for the fiber diameter distribution

(a)	Diameter (μm)	4.9 – 5.7		5.7 – 6.5		6.5 – 7.3		7.3 – 8.1	
	Fraction (%)	5.7 ± 0.2		20.7 ± 0.1		56.6 ± 0.5		17.0 ± 0.3	
(b)	Diameter (μm)	0 – 1.4	1.4 – 2.8	2.8 – 4.2	4.2 – 5.6	5.6 – 7.0	7.0 – 8.4	8.4 – 9.8	
	Fraction (%)	2.1 ± 0.1	14.6 ± 0.4	14.6 ± 0.2	16.7 ± 0.2	25.0 ± 0.5	22.9 ± 0.3	4.1 ± 0.3	
(c)	Diameter (μm)	0 – 1.7	1.7 – 3.4	3.4 – 5.1	5.1 – 6.8	6.8 – 8.5	8.5 – 10.2	10.2 – 11.9	
	Fraction (%)	6.9 ± 0.3	10.3 ± 0.5	24.1 ± 0.2	36.2 ± 0.2	15.5 ± 0.1	3.5 ± 0.4	3.5 ± 0.3	
(d)	Diameter (μm)	0 – 1.4	1.4 – 2.8	2.8 – 4.2	4.2 – 5.6	5.6 – 7.0	7.0 – 8.4	8.4 – 9.8	9.8 – 11.2
	Fraction (%)	5.2 ± 0.2	24.7 ± 0.2	20.8 ± 0.3	15.6 ± 0.1	27.7 ± 0.4	2.5 ± 0.3	1.0 ± 0.5	2.5 ± 0.3

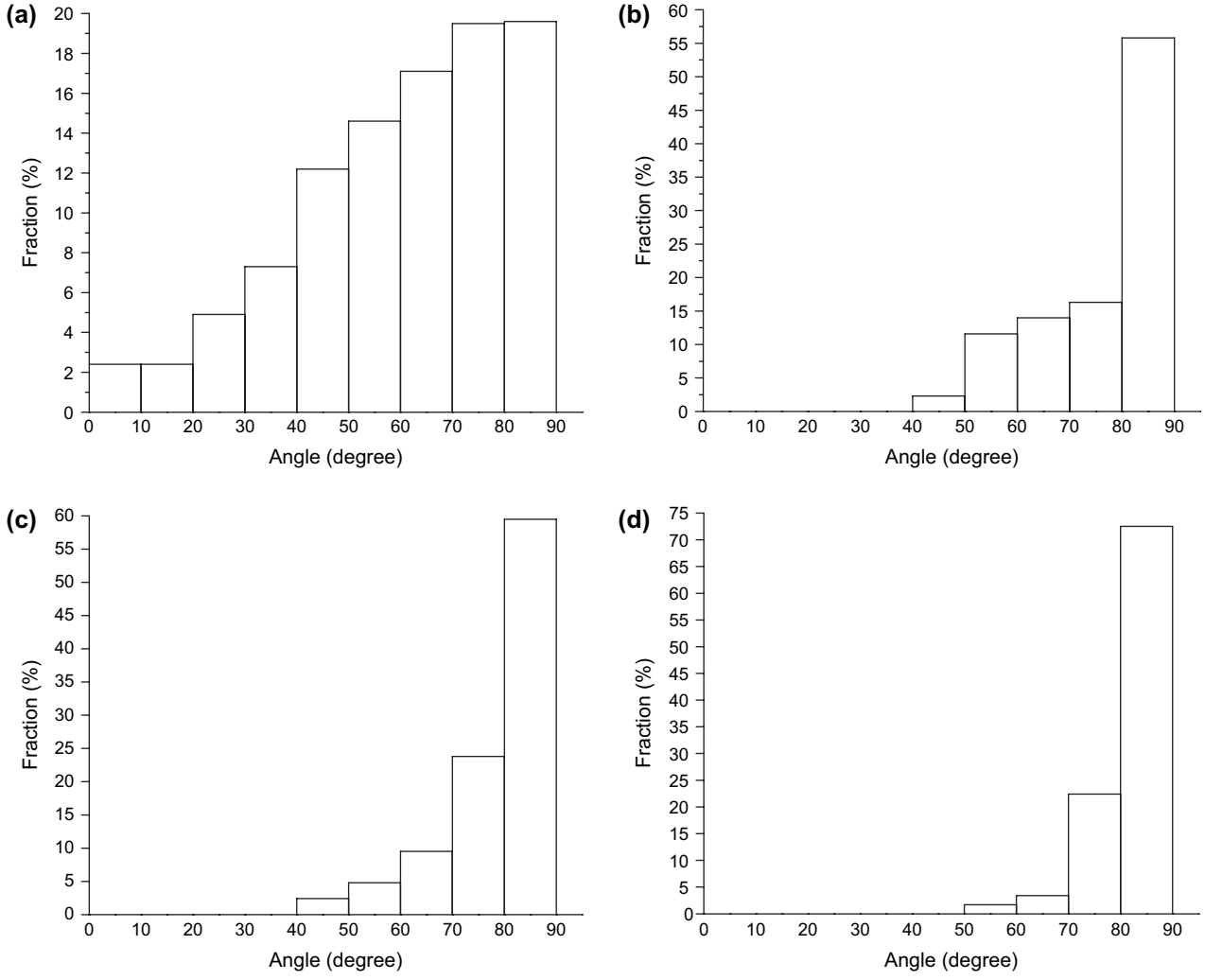

Fig. 7. Fiber aligned angle distributions of mats prepared with differently designed electrodes: (a) no auxiliary electrodes; (b) one counter auxiliary electrode; (c) and (d) three auxiliary electrodes with different separation distances.

without applying any auxiliary electrodes. When one counter auxiliary electrode was used to focus and align the electrospun fibers, the fiber alignment was enhanced, as shown in Fig. 8(b). When three auxiliary electrodes were employed to align and narrow the electrospun mat, a good alignment of electrospun fibers was achieved, as shown in Fig. 8(c). This behavior was attributed to the converged electric field that helped to align and narrow the nanometer-scale electrospun PCL fibers. It was concluded from this experiment that the auxiliary electrodes can focus and align not only micrometer-scale electrospun fibers, but also nanometer-scale electrospun fibers.

Fig. 9(a) and (b) shows SEM images at the boundary of the electrospun PCL mats prepared without applying auxiliary electrodes and by applying three auxiliary electrodes, respectively. The micrographs reveal that the microstructure at the boundary of the mats was similar to that at the center of the mats, as shown in Fig. 5(a) and (c). The electrospun PCL fibers were distributed randomly at the boundary without employing auxiliary electrodes whereas the fibers were aligned along one direction at the boundary when employing three auxiliary electrodes. The electrospun fibers were aligned and converged in the auxiliary electrode configuration because the electrospun fibers followed the electric field lines in

Table 4
Standard deviation of the fraction for the aligned angle distribution

	0°–10°	10°–20°	20°–30°	30°–40°	40°–50°	50°–60°	60°–70°	70°–80°	80°–90°
(a)	2.4 ± 0.1	2.4 ± 0.3	4.9 ± 0.1	7.3 ± 0.3	12.2 ± 0.4	14.6 ± 0.5	17.1 ± 0.2	19.5 ± 0.4	19.6 ± 0.1
(b)	0	0	0	0	2.3 ± 0.3	11.6 ± 0.5	14.0 ± 0.2	16.3 ± 0.4	55.8 ± 0.4
(c)	0	0	0	0	2.4 ± 0.2	4.8 ± 0.2	9.5 ± 0.5	23.8 ± 0.1	59.5 ± 0.3
(d)	0	0	0	0	0	1.7 ± 0.5	3.4 ± 0.2	22.4 ± 0.1	72.5 ± 0.4

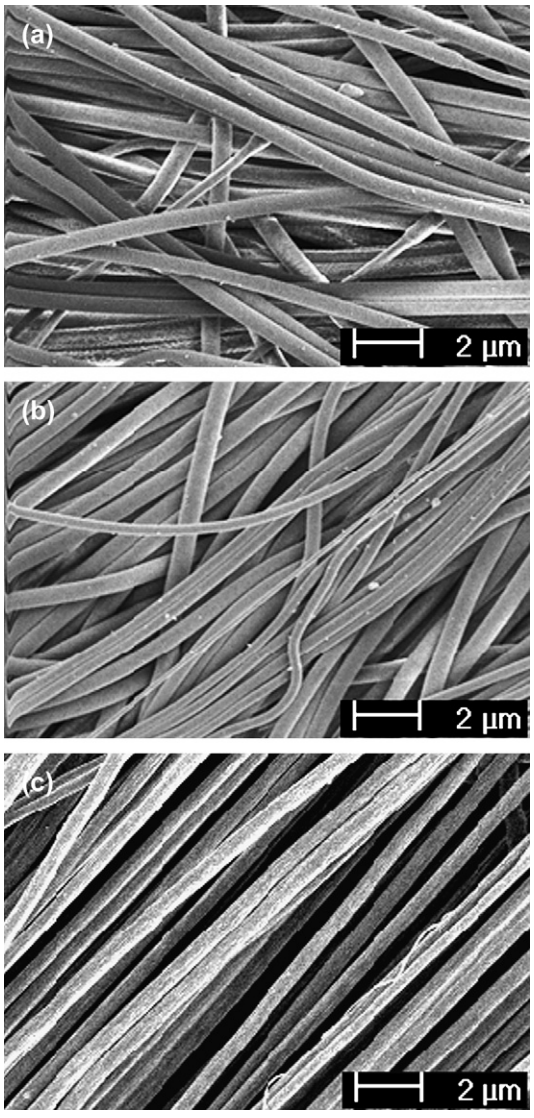

Fig. 8. SEM images of nanostructured electrospun mats prepared with differently designed electrodes: (a) no auxiliary electrodes; (b) one counter auxiliary electrode and (c) three auxiliary electrodes.

the converged fashion. When they reached the drum collector, the converged fibers were parallelly taken-up by the collector to form alignment structure in a narrow region. This demonstrates that the electrospun PCL fibers in the mats have similar distribution microstructure at the boundary and center.

In an effort to control fiber alignment and width of the electrospun mat, three auxiliary electrodes were employed simultaneously in the presence of a rotating drum collector. The experimental data demonstrated that the auxiliary electrodes helped in converging the electrospun fibers and exerting an aligning force on the electrospun fibers. To understand the mechanism of the alignment and distribution of electrospun fibers using the three auxiliary electrodes, the electric field strength vectors were modeled and plotted. The rationale for the shape of the electric field is that any positive or negative electrode will create an electric field surrounding it, and the magnitude and direction of the electric field at each location is the result of the electric field vectors for the individual charges within the configuration. However, the electric field lines will never cross each other, and the density of lines at a specific location represents the strength of the electric field. The strength of an electric field is directly related to the quantity of electrode charge and inversely related to the distance from the electrodes. When the electrodes posses the same amount of charge, the electric field pattern will be symmetrical in configuration. Fig. 10 illustrates a cross-sectional view of the direction and field strength of the macroscopic electric field vectors between the nozzle and the auxiliary electrodes generated by the apparatus used in this experiment. The electric field is almost uniform along the collector without employing any auxiliary electrodes. Therefore, the fibers that were deposited along the collector under this electrostatic force resulted in a large deposition area. When the auxiliary electrodes were used to assist the alignment, there was a tendency for the field lines near the nozzle to be converged and the electric field lines in the vicinity of the collector converge toward the opposite electrode. Under the influence of converging electric field lines, fibers can be collected in higher density (small deposition area) near the center of the collector.

4. Conclusion

We have demonstrated a simple and efficient method for controlling the width of electrospun fiber mats, incorporating

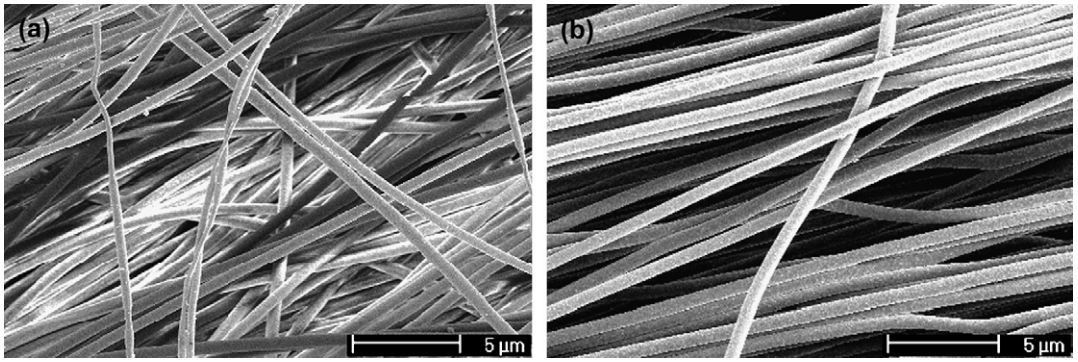

Fig. 9. SEM images at the boundaries of the nanostructured electrospun mats generated with (a) no auxiliary electrodes and (b) three auxiliary electrodes.

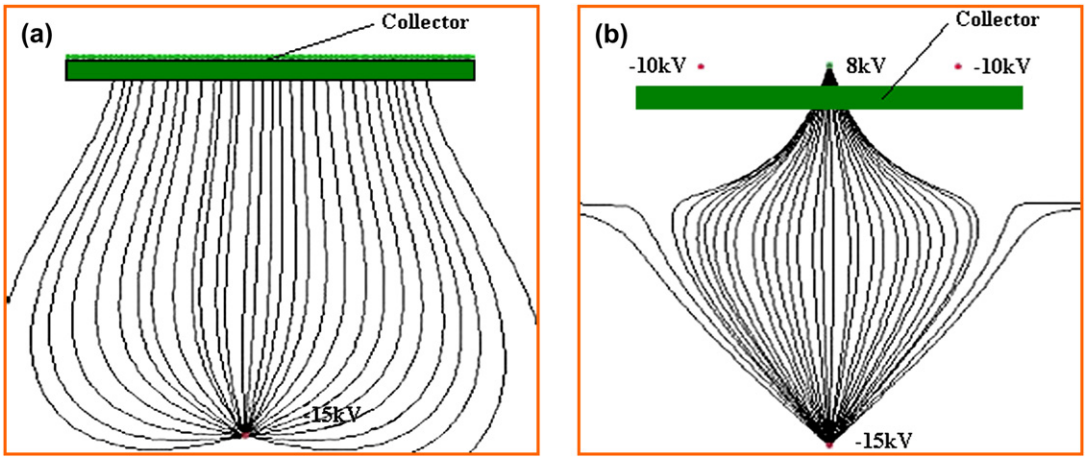

Fig. 10. Simulations of calculated electric field strength vectors in the region between the nozzle and the collector: (a) without auxiliary electrodes and (b) with one positive and two negative auxiliary electrodes.

aligned features through both mechanical and electrical means. The alignment of the electrospun fibers in a micrometer and nanometer scale was achieved by stretching and converging the fibers through the use of an electrostatic field generated with an array of auxiliary electrodes. The microstructure and alignment angles of these fibers were characterized and compared with that of fibers produced without the use of auxiliary electrodes. The experimental results reveal that the percentage of the aligned angle of the micrometer fibers scattered in the range of 80°–90° increased from 19.6% for electrospun mats prepared without any auxiliary electrodes, to a value of 72.5% for mats produced using three auxiliary electrodes. When the distance between auxiliary electrodes was decreased, the resulting electrospun fibers were more perpendicular to the axis of the collector and displayed increased fiber distribution density. The assembly density of the fibers increased from 2.0 N/cm, when no auxiliary electrodes were incorporated, to 4.2 N/cm when three auxiliary electrodes were incorporated. The electrospun fibers at the boundary had the same distribution patterns as those in the center of the electrospun mats. The alignment effect does not be changed when the electrospun fibers are in nanometer scale. These results are specific to the geometries of the current setup, but clearly display the potential for controlling fiber mat density through the use of auxiliary electrode arrays. It was further noted that the auxiliary electrodes had no profound effects on the average diameters of fibers. Based upon the results presented, the modified electrospinning process appears to have significant potential for fabrication of highly oriented micrometer or nanometer fibers over controlled areas of deposition.

References

[1] Huang ZM, Zhang YZ, Kotaki M, Ramakrishna S. Compos Sci Technol 2003;63:2223.
[2] Li D, Xia YN. Adv Mater 2004;16:1151.
[3] Reneker DH, Chun I. Nanotechnology 1996;7:216.
[4] Nair LS, Bhattacharyya S, Laurencin CT. Expert Opin Biol Ther 2004;4:659.
[5] Pham QP, Sharma U, Mikos AG. Tissue Eng 2006;12:1197.
[6] Pan H, Li LM, Hu L, Cui XJ. Polymer 2006;47:4901.
[7] Dai HQ, Gong J, Kim H, Lee D. Nanotechnology 2002;13:674.
[8] Yoon KH, Kim KS, Wang XF, Fang DF, Hsiao BS, Chu B. Polymer 2006;47:2434.
[9] Matthews JA, Wnek GE, Simpson DG, Bowlin GL. Biomacromolecules 2002;3:232.
[10] Murugan R, Ramakrishna S. Tissue Eng 2006;12:435.
[11] Kim J, Jia HF, Wang P. Biotechnol Adv 2006;24:296.
[12] Jose MV, Steinert BW, Thomas V, Dean DR, Abdalla MA, Price G, et al. Polymer 2007;48:1096.
[13] Qin XH, Wang SY. J Appl Polym Sci 2006;102:1285.
[14] Wang XY, Drew C, Lee SH, Senecal KJ, Kumar J, Samuelson LA. J Macromol Sci Pure Appl Chem 2002;39:1251.
[15] Ramakrishna S, Fujihara K, Teo WE, Yong T, Ma ZW, Ramaseshan R. Mater. Today 2006;9:40.
[16] Doshi J, Reneker DH. J Electrostat 1995;35:151.
[17] Ganan-Calvo AM. Phys Rev Lett 1997;79:217.
[18] Reneker DH, Yarin AL, Fong H, Koombhongse S. J Appl Phys 2000;87:4531.
[19] Xu CY, Inai R, Kotaki M, Ramakrishna S. Biomaterials 2004;25:877.
[20] Li D, Wang YL, Xia YN. Nano Lett 2003;3:1167.
[21] Dharmaraj N, Park HC, Kim CH, Viswanathamurthi P, Kim HY. Mater Res Bull 2006;41:612.
[22] Wang A, Singh H, Hatton TA, Rutledge GC. Polymer 2004;45:5505.
[23] Kameoka J, Orth R, Yang YN, Czaplewski D, Mathers R, Coates GW, et al. Nanotechnology 2003;14:1124.
[24] Yang F, Murugan R, Wang S, Ramakrishna S. Biomaterials 2005;26:2603.
[25] Katta P, Alessandro M, Ramsier RD, Chase GG. Nano Lett 2004;4:2215.
[26] Sundaray B, Subramanian V, Natarajan TS, Xiang RZ, Chang CC, Fann WS. Appl Phys Lett 2004;84:1222.
[27] Wang G, Tan ZK, Liu XQ, Chawda S, Koo JS, Samuilov V, et al. Nanotechnology 2006;17:5829.
[28] Theron A, Zussman E, Yarin AL. Nanotechnology 2001;12:384.
[29] Li D, Ouyang G, McCann JT, Xia YN. Nano Lett 2005;5:913.
[30] Li D, Wang YL, Xia YN. Adv Mater 2004;16:361.
[31] Carnell LS, Holloway NM, Stephens R, Siochi EJ, Clark RL. in preparation.
[32] Deitzel JM, Kleinmeyer JD, Hirvonen JK, Tan NCB. Polymer 2001;42:8163.